REPORT DOCUMENTATION PAGE

Form Approved
OMB No. 0704-0188

1. AGENCY USE ONLY *(Leave blank)*	2. REPORT DATE	3. REPORT TYPE AND DATES COVERED
	March 31, 1998	Final

4. TITLE AND SUBTITLE
DI Diesel Performance and Emissions Model

5. FUNDING NUMBERS
DAAH04-94-G-0236

6. AUTHORS
Mellor, A.M., Easley, W.L., Mello, J.P. and Psota, M.A.

7. PERFORMING ORGANIZATION NAME(S) AND ADDRESS(ES)
Vanderbilt University
Box 1592, Station B
Nashville, TN 37205-1592

8. PERFORMING ORGANIZATION REPORT NUMBER

9. SPONSORING/MONITORING AGENCY NAME(S) AND ADDRESS(ES)
U.S. Army Research Office
P.O. Box 12211
Research Triangle Park, N.C. 27709-2211

10. SPONSORING/MONITORING AGENCY REPORT NUMBER
ARO 32535.6-EG

11. SUPPLEMENTARY NOTES
The views, opinions and/or findings contained in this report are those of the author(s) and should not be construed as an official Department of the Army position, policy or decision, unless so designated by other documentation.

12a. DISTRIBUTION/AVAILABILITY STATEMENT
Approved for public release; distribution unlimited.

19980520 053

13. ABSTRACT *(Maximum 200 words)*

Based on findings indicating that both the Zeldovich and N_2O mechanisms are important in the formation and decomposition of NO in direct injection (DI) Diesel engines, a skeletal mechanism consisting of seven elementary reactions is used to develop a two-zone model for NO_x emissions from DI Diesel engines. Characteristic chemical kinetic times for NO formation in zone 1 and NO decomposition in zone 2 are formulated from the law of mass action applied separately to each zone, and the relative importance of NO decomposition in four DI Diesel engines is examined. Preliminary fluid mechanic mixing times for NO formation are developed by the combination of fluid relations characteristic of each of the many mixing processes occurring in a DI Diesel engine. These results are empirical, but future fluid mechanic mixing times applicable to all DI Diesel engines may be found. Similarly, a two-zone soot CTM accounting for both soot formation and oxidation is outlined. The NO_x/soot tradeoff for low loads is also proven using the preliminary models for soot and NO_x thereby showing that when complete the models will predict the correct trends.

14. SUBJECT TERMS	15. NUMBER OF PAGES
DI Diesel emission models, combustion processes, skeletal mechanisms, NO_x, and soot.	41
	16. PRICE CODE

17. SECURITY CLASSIFICATION OF REPORT	18. SECURITY CLASSIFICATION OF THIS PAGE	19. SECURITY CLASSIFICATION OF ABSTRACT	20. LIMITATION OF ABSTRACT

TABLE OF CONTENTS

NOMENCLATURE

bmep	Brake mean effective pressure (kPa)
bsfc	Brake specific fuel consumption (g/kW-hr)
CTM	Characteristic time model
Da	Damköhler number
d_{noz}	Nozzle hole diameter (m)
E	Activation energy (cal/gmol)
EGR	Exhaust gas recirculation
K_c	Equilibrium constant based on concentration
k_{if}	Forward rate coefficient of the *i*th reaction
k_{ir}	Reverse rate coefficient of the *i*th reaction
l_{imp}	Fuel jet impingement distance (m)
M_{NO2}	Molecular weight of NO_2
m	Model constant incorporating various conversion constants
m_f	Mass of fuel per cycle (g)
m_{sf}	Model constant for soot formation process
m_{so}	Model constant for soot oxidation process
m′	Scale factor
N	Engine speed (rpm)
NO_xEI	Oxides of nitrogen emissions index (g NO_x as NO_2/kg fuel)
P_2	Cylinder pressure at start of combustion (atm)
P_3	Maximum cylinder pressure (atm)
PSR	Perfectly stirred reactor
R	Universal gas constant (1.986 cal/gmol·K or 82.06 atm L/kmol·K); correlation coefficient

Re	Reynolds number
R*i*	*i*th reaction in a mechanism
r_c	Compression ratio
SootEI	Soot emissions index (g soot/kg fuel)
T_2	Cylinder temperature at start of combustion (K)
T_{3b}	Burned gas temperature at the end of combustion (K)
$T_{50\%}$	50% fuel recovery temperature (K)
$T_{\phi=1}$	Stoichiometric, adiabatic flame temperature (K)
$T_{\phi=3}$	Temperature at a equivalence ratio of 3 (K)
V_{3b}	Cylinder volume at the end of combustion (cm^3)
We	Weber number
ΔP	Pressure drop across fuel injection nozzle (MPa)
ε_{NO}	Fractional extent of reaction for NO formed per eddy in a given zone
ϕ	Fuel-air equivalence ratio
ρ_a	Density of air
ρ_d	Power density
$\tau_{fi,no}$	Eddy lifetime in NO formation zone
τ_{id}	Characteristic time for ignition delay
τ_{imp}	Characteristic time for fuel impingement on cylinder bowl wall (based on the penetration correlation of Arai and Hiroyasu (1990)
τ_{no}	Characteristic kinetic time for NO formation (s or ms)
$\tau_{no,3b}$	Characteristic kinetic time for NO decomposition (s or ms)
τ_{sf}	Characteristic kinetic time for soot formation (s or ms)
$\tau_{sl,3b}$	Eddy lifetime in NO decomposition zone
$\tau_{sl,sf}$	Eddy lifetime in soot formation zone

$\tau_{sl,so}$	Eddy lifetime in soot oxidation zone
τ_{so}	Characteristic kinetic time for soot oxidation (s or ms)
υ_{fuel}	Kinematic viscosity of fuel

Subscripts:

eq	Equilibrium
f	Forward reaction
no	Nitric oxide
ov	Overall equivalence ratio
r	Reverse reaction
sf	Soot formation
so	Soot oxidation
$\phi = 1$	Stoichiometric
∞	High-pressure limit
0	Low-pressure limit
1	Zone 1 conditions
1′	Zone 1′ conditions
2	Zone 2 conditions
3b	End of combustion

LIST OF FIGURES

LIST OF TABLES

1.0 CHARACTERISTIC TIME MODEL

1.1 STATEMENT OF THE PROBLEM STUDIED

The goal of this work has been to develop characteristic time models (CTMs) for the prediction of engine-out NO_x and soot emissions from direct injection (DI) Diesel engines. The CTM approach to emission prediction involves identifying the characteristic times of the dominant chemical and fluid mechanic subprocesses in the combustion phenomenon and, based on these times, develop a correlation between the appropriate model and pollutant. From a computational standpoint, this type of semi-empirical correlation is relatively simple. Consequently, the model is useful as a preliminary design tool, which may be used by Diesel engineers to reduce the cycle time required to design, develop and test new engines. The computational simplicity of the model also makes it amenable to incorporation into a CFD code or a phenomenological cycle simulation code to improve the emissions prediction. Still another perceived end use is for real-time engine emissions control.

In previous work done to model NO_x emissions in Diesel engines, Ahmad and Plee (1983) showed that NO kinetics are described by a single global activation temperature. The global activation temperature suggested by these investigators for DI Diesels was 34,300 K, significantly less than the global activation temperature that is typically associated with NO formation through the extended Zeldovich kinetics in conventional gas turbine combustors (68,479 K, Sawyer et al., 1973; 67,976 K, Tuttle et al., 1977). Ahmad and Plee (1983) attribute this difference to NO decomposition within the engine. Thus, the model of Ahmad and Plee (1983) implies that the importance of NO decomposition relative to formation in Diesel combustion is approximately constant.

More recent analysis by Duffy et al. (1996), however, suggests that a single global activation temperature does not model NO_x emissions from modern DI Diesel engines. Consequently, the one-step global model of Ahmad and Plee (1983), though adequate for the engines analyzed in that investigation, is not generally applicable to DI Diesel engines.

The work of Plee and coworkers (Plee et al., 1981; Ahmad and Plee, 1983) also used a single global activation temperature to describe the kinetics of particulate emissions. The obtained activation temperature represented the contributions of both soot oxidation and formation, and varied from engine to engine. The variations of the activation temperature was attributed to differences in mixing and thus combustion chamber geometry. The increased mixing causes the formation of soot to be reduced along with better recirculation of soot particles through the reaction zone, enhancing soot oxidation (Ahmad and Plee, 1983). Although both chemical processes involved in soot emissions are important, it was concluded that the oxidation process is dominant and affected more by flame temperature changes.

In this work, the one-step global approach to modeling NO kinetics in Diesels is replaced by a skeletal mechanism, which contains the NO chemistry relevant to high pressure and temperature combustion typical of DI Diesels. Additionally, based on the work done under this program as well as laser-sheet imaging results from Dec (1997), a zonal model of the physics of the NO formation and decomposition processes in Diesels is postulated. From these kinetic and physical models for NO emissions, a characteristic time model for NO_x emissions from Diesel engines is derived. From kinetic times for NO formation and decomposition, derived here from first principles, the factors affecting

the importance of NO decomposition are evaluated. Preliminary empirical analysis to define a fluid mechanic time for NO formation has also been performed under this program.

For the soot emissions model, the global activation temperature approach still applies, but the contribution of both soot formation and oxidation will be represented by individual chemical kinetic and mixing times. Also based on the work of Dec (1997), a two zone model is postulated for soot with the importance of each chemical process dependent on the spatial location.

1.2 SKELETAL MECHANISM FOR NO CHEMISTRY

NO_x chemistry can proceed through the extended Zeldovich mechanism (Lavoie et al., 1970), the prompt mechanism (Fenimore, 1971), the N_2O mechanism (Malte and Pratt, 1974), and NO formation from fuel-bound nitrogen. The last pathway is negligible for modern Diesel fuels, which contain low amounts of organic nitrogen.

To formulate a skeletal mechanism for NO_x emissions in Diesel engines, it is necessary to consider the different pathways of NO formation and decomposition and, through kinetic analysis, determine those pathways that are significant at the operating conditions of interest. Mellor et al. (1998) present a review of such kinetic analyses. From this review it is concluded that, at conditions typical of Diesel combustion (i.e., stoichiometric and lean flame temperatures and high pressures), the significant paths for NO chemistry are the extended Zeldovich (Lavoie et al., 1970) and nitrous oxide (Malte and Pratt, 1974) mechanisms.

Based on the review discussed above, Mellor et al. (1998) postulate a skeletal mechanism for NO chemistry in DI Diesel engines. This mechanism is expressed as

$$O + N_2 \Leftrightarrow NO + N \qquad (R1)$$

$$N + O_2 \Leftrightarrow NO + O \qquad (R2)$$

$$N + OH \Leftrightarrow NO + H \qquad (R3)$$

$$N_2O + O \Leftrightarrow 2NO \qquad (R4)$$

$$O + N_2 + M \Leftrightarrow N_2O + M \qquad (R5)$$

$$O_2 + M \Leftrightarrow 2O + M \qquad (R6)$$

$$N_2O + M \Leftrightarrow NO + NH... \Rightarrow 2NO \qquad (R7)$$

where reactions (R1), (R2), (R3), and (R6) are from the extended Zeldovich mechanism and (R4), (R5), and (R7) are from the N_2O mechanism.

Along with the kinetic studies reviewed by Mellor et al. (1998), the present exclusion of the prompt mechanism at Diesel conditions is further supported by Dec (1997). Using laser-sheet imaging, he shows that premixed combustion in DI Diesels is not conducive to NO formation through the prompt mechanism since $\phi \approx 4$. Dec (1997) does argue that prompt NO may form in the diffusion portion of the Diesel burning process; nevertheless, given the temperature of Diesel combustion, NO formation through this pathway is likely to be negligible compared to the alternatives.

It is also important to note that (R5) is a three-body reaction and is thus pressure sensitive. In the following section, it will be shown that this pressure sensitivity changes the relative contribution of the N_2O pathway to NO formation in Diesel engines.

1.3 TWO-ZONE MODEL FOR DIESEL COMBUSTION

Based on recent laser sheet imaging results of Dec (1997) and the earlier findings of Ahmad and Plee (1983), Mellor et al. (1998) have postulated a two-zone model for NO formation and decomposition in DI Diesel engines as illustrated in Fig. 1-1. In the figure,

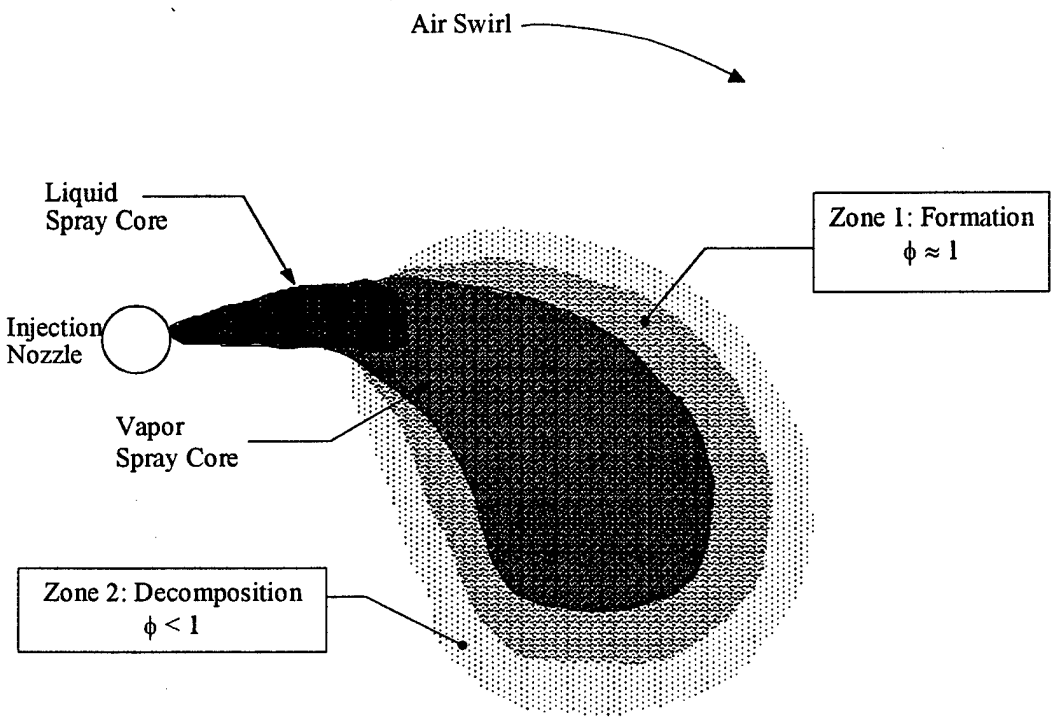

Figure 1-1. The two-zone model for NO formation and decomposition in a DI Diesel combustion chamber as postulated by Mellor et al. (1998). Zone 1′ is intermediate and based on the zone 1 pressure and flame temperature but the zone 2 stoichiometry, ϕ_{ov}, for the engine.

Zone 1 is a near stoichiometric region ($\phi \approx 1$) where [NO] is small and in which NO formation occurs through forward reactions (R1) through (R5), equilibrium (R6), and forward reaction (R7). Following the results of Dec (1997), this zone is shown as a thin layer surrounding the periphery of the fuel plume. Between zone 1 and zone 2, there is a transition in which the concentrations of the products in zone 1 are adjusted to the overall engine stoichiometry (zone 1′). Zone 2 is a region in which hot, burned gases are present at the overall equivalence ratio. In this zone, NO decomposition occurs through the reverse of the mechanism given above.

The adiabatic stoichiometric flame temperature $T_{\phi=1}$ for zones 1 and 1′ is computed following Plee et al. (1980), that is, with start of combustion (SOC) conditions, the stoichiometric amount of fuel, and assuming constant pressure burning. Stoichiometric temperatures vary from 2200 K to 2700 K with the lower values resulting from EGR or water injection. The representative temperature in zone 2 is the end of combustion temperature, T_{3b} and is calculated following Mellor et al. (1998). Typical values for T_{3b} are in the range of 1300 to 2200 K depending upon overall equivalence ratio, inlet manifold conditions, and so forth.

In the zonal model just described, it is assumed that concentration and temperature gradients can be ignored within a given zone. Thus, Mellor et al. (1998) model the chemistry in each zone using a perfectly stirred reactor (PSR) simulation (Bowman et al., 1995) with adiabaticity assumed. The GRI MECH 2.11 methane-air kinetic mechanism (Bowman et al., 1995) is used to provide heat release and, in this sense, model stoichiometric and lean Diesel fuel combustion.

The relatively constant concentrations of N-atom and N_2O in each zone provide a basis for the steady-state approximation to be made in the following section. Also, the PSR simulation of Mellor et al. (1998) shows that $[NO]_{eq}$ is largest in zone 1′ where $\phi = \phi_{ov}$ and the reactor temperature and pressure remain at the stoichiometric zone conditions. This fact will be used in the definition of the characteristic times derived below.

1.4 NO FORMATION AND DECOMPOSITION TIMES

1.4.1 Characteristic Time For NO Formation

Writing the law of mass action for the rate of NO formation in zone 1 gives

$$d[NO]/dt = k_{1f}[O][N_2] + k_{2f}[N][O_2] + k_{3f}[N][OH] + 2k_{4f}[N_2O][O] + 2k_{7f}[N_2O][H] \quad (1)$$

Invoking the N-atom and N_2O steady state assumptions as discussed above, Eq. (1) becomes

$$d[NO]/dt = 2[O][N_2](k_{1f} + k_{5f}) \quad (2)$$

The NO-forming eddies, to which Eq. (2) applies, originate just inside zone 1 and are convected outward through zone 1′ to zone 2.

Mellor et al. (1998) let ε_{NO} represent the fractional extent of reaction of NO such that $\varepsilon_{NO} = [NO]/[NO]_{eq1'}$ where $0 < \varepsilon_{NO} < 1$ and $[NO]_{eq1'}$ is the equilibrium NO concentration from the zone 1 stoichiometric flame temperature calculation adjusted to the overall engine stoichiometry. As shown by Mellor et al. (1998), $[NO]_{eq1'}$ is the proper choice as a normalizing factor to constrain ε_{NO} between the limits of zero and one since it is the largest value among the various zones.

Substituting this definition into Eq. (2) gives

$$d\varepsilon_{NO}/dt = (1/[NO]_{eq1'})(d[NO]/dt) = 2[O][N_2](k_{1f} + k_{5f})/[NO]_{eq1'} \quad (3)$$

The inverse of this equation is the characteristic time for NO formation

$$\tau_{no} = [NO]_{eq1'} / (2[O]_{eq1}[N_2]_{eq1} (k_{1f} + k_{5f})) \quad (4)$$

where $[O]_{eq1}$, $[N_2]_{eq1}$, and the rate coefficients are evaluated at the zone 1 burned gas conditions (i.e., the output from the stoichiometric equilibrium calculation based on motored engine conditions at start of combustion).

Also, Mellor et al. (1998) define Zeldovich and N_2O mechanism formation times as follows:

$$\tau_{no,1f} = [NO]_{eq1'}/2k_{1f}[O]_{eq1}[N_2]_{eq1} \quad (5)$$

$$\tau_{no,5f} = [NO]_{eq1'}/2k_{5f}[O]_{eq1}[N_2]_{eq1} \quad (6)$$

The activation temperatures for $\tau_{no,5f}$ and $\tau_{no,1f}$ are 36120 K and 62184 K, respectively. The latter value is typical of the values obtained for NO_x emissions from conventional gas turbine combustors (see the discussion above).

Recall that k_{1f}, in Eq. (4) and (5), represents the extended Zeldovich mechanism, (R1) through (R3), while the k_{5f} term in Eq. (4) and (6) is the third-body component, thus sensitive to pressure, originating in the N_2O mechanism, (R4), (R5), and (R7). In Fig. 1-2 each contribution in Eq. (2) is evaluated in Arrhenius format for typical engine conditions using the kinetic information presented in Mellor et al. (1998).

The figure shows that at low pressures, 1 or 10 atm, NO formation will follow extended Zeldovich kinetics (k_{1f} exceeds k_{5f}) over most of the temperature range shown. However, at 10 atm and the lower stoichiometric flame temperatures, obtained with inert injection for example, the N_2O mechanism will be predominant (k_{5f} exceeds k_{1f}). The crossover temperature moves to somewhat higher values as the pressure is increased, and for 60 atm (representative of motored TDC Diesel conditions), the N_2O mechanism dominates at many stoichiometric temperatures of interest (approximately 2200 to 2460

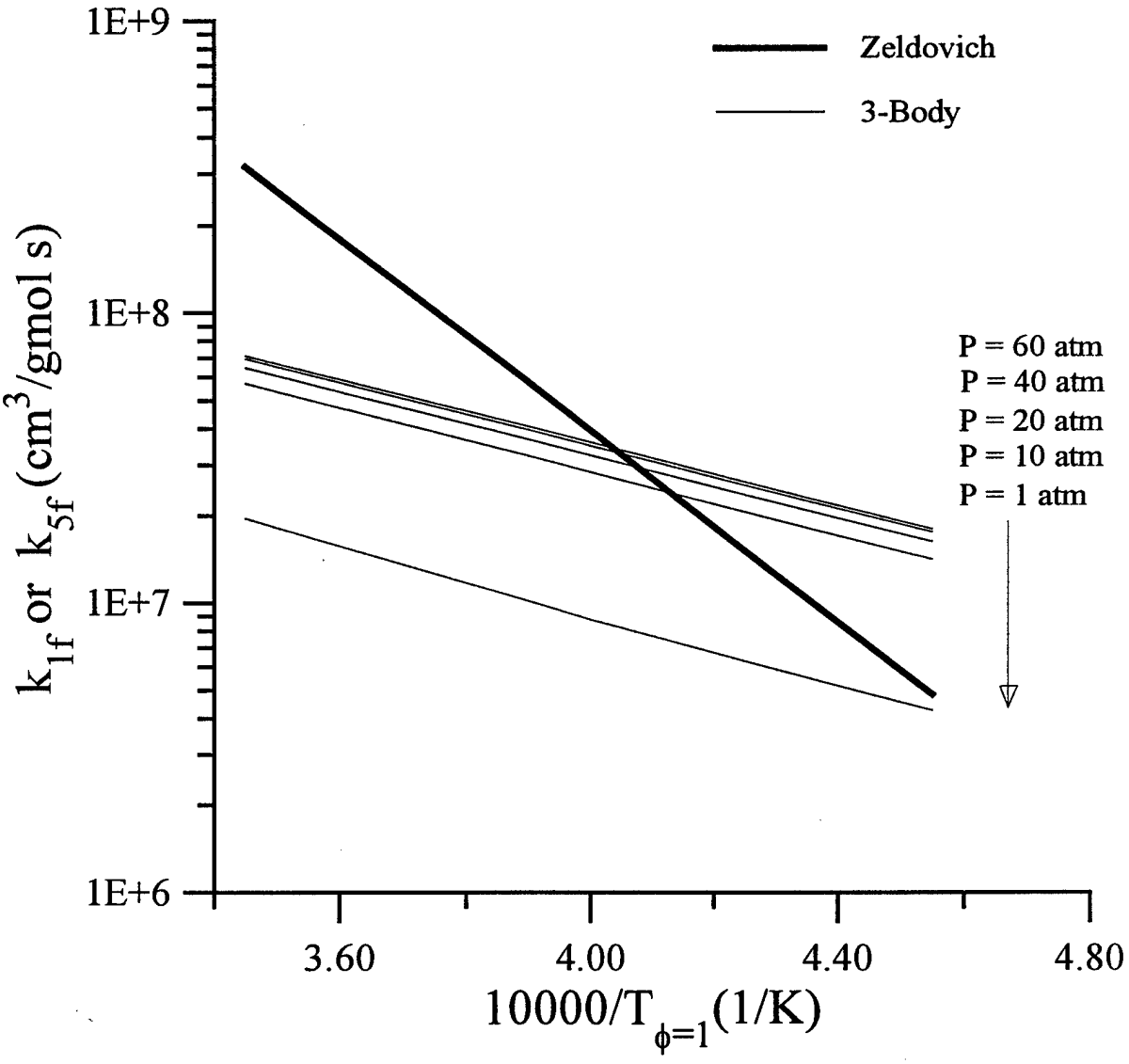

Figure 1-2. The contribution of the Zeldovich and N_2O mechanisms to the NO formation rate as postulated by Mellor et al. (1998). The information in this figure is presented in Arrhenius format for typical engine conditions. Logarithms are presented as functions of inverse stoichiometric flame temperature in the approximate range from 2200 to 2900 K, so that midrange values correspond to stoichiometric values, with pressure as a parameter.

K). The contribution of this mechanism at higher values of stoichiometric temperature can not be ignored.

1.4.2 Characteristic Time for NO Decomposition

The characteristic time for NO decomposition is defined in a manner analogous to the characteristic time for NO formation. Writing the law of mass action for the rate of NO decomposition in zone 2 gives (for reasons given by Mellor et al. (1998), the reverse of (R7) is ignored for the present analysis)

$$d[NO]/dt = - k_{1r}[NO][N] - k_{2r}[NO][O] - k_{3r}[NO][H] - 2k_{4r}[NO]^2 \quad (7)$$

Expressed in terms of the fractional extent of reaction, and again assuming steady-state N-atom, this equation becomes

$$d\varepsilon_{NO}/dt = (1/[NO]_{eq1'})(d[NO]/dt) = (- 2k_{1r}[NO][N] - 2k_{4r}[NO]^2)/[NO]_{eq1'} \quad (8)$$

The inverse of this expression is the characteristic time for NO decomposition

$$\tau_{no,3b} = 1/ [\varepsilon_{NO} (2k_{1r} [N]_{eq2} + 2k_{4r}[NO]_{eq1'}\varepsilon_{NO})] \quad (9)$$

The form of this equation demonstrates that NO decomposition is a function of both the reverse Zeldovich mechanism ($2k_{1r}[N]_{eq2}$) and the reverse N_2O mechanism ($2k_{4r}[NO]_{eq1'}\varepsilon_{NO}$). Individual decomposition times for the extended Zeldovich and N_2O mechanisms are respectively expressed as

$$\tau_{3b,1r} = 1/2k_{1r}[N]_{eq2} \quad (10)$$

$$\tau_{3b,4r} = 1/2k_{4r}[NO]_{eq1'} \quad (11)$$

In an Arrhenius plot similar to Fig. 1-2, Mellor et al. (1998) show that NO decomposition through the reverse N_2O mechanism is dominant over a range of typical DI Diesel operating conditions (p = 60 atm and T_{3b} = 1300 K to 2200 K).

1.5 CHARACTERISTIC TIME MODEL FOR NO_X FROM DIESEL ENGINES

Using the kinetic times defined above, expressions for the engine-out NO_x emissions are obtained by integrating the laws of mass action over the fluid or residence times available in zones 1-1′ and 2. For NO formation in zones 1-1′, Eq. (3) and (4) are combined such that

$$d\varepsilon_{NO}/dt = 1/\tau_{no} \tag{11}$$

where [O] and $[N_2]$ in τ_{no} are evaluated at constant equilibrium zone 1 conditions. Equation (11) can be integrated over the eddy lifetime in zone 1-1′, $\tau_{fi,no}$, to obtain

$$\varepsilon_{NO1'} = m'(\tau_{fi,no}/\tau_{no}) = m'Da_{no} \tag{12}$$

In Eq. (12), $\varepsilon_{NO1'}$ is the fractional extent of reaction for NO formed in zone 1-1′ per stoichiometric eddy, m′ is a scale factor introduced because the magnitude of the characteristic time ratio is unknown at this point, and Da_{no} is the Damköhler number for NO formation in zone 1-1′.

If a portion of the NO formed in zone 1-1′ decomposes in zone 2, then as Mellor et al. (1998) have shown in detail, Eq. (8), (10), and (11) can be used to obtain engine-out emissions such that

$$NO_xEI = \frac{m\dfrac{V_{3b}}{m_f}Da_{no}[NO]_{eq1'}e^{-Da_{3b,1r}}}{1+\varepsilon_{NO1'}\dfrac{k_{4r}[NO]_{eq1'}}{k_{1r}[N]_{eq2}}\left(1-e^{-Da_{3b,1r}}\right)} \tag{13}$$

where m is a model constant incorporating the scaling factor m′ and other conversion constants, $Da_{3b,1r}$ is a Damköhler number based on the eddy lifetime in zone 2 ($\tau_{sl,3b}$) and the reverse Zeldovich mechanism for zone 2 ($Da_{3b} \equiv \tau_{sl,3b}/\tau_{3b,1r}$), m_f is the fuel supplied

per cycle in g, and V_{3b} is the volume in the cylinder at the end of combustion in cm^3.

Mellor et al. (1998) show that Eq. (13) can be simplified for various limiting cases. In particular, if the eddy lifetime in zone 2 is inadequate so that NO decomposition is negligible (i.e., $\tau_{sl,3b}$ and $Da_{3b,1r}$ approach zero), then

$$NO_xEI = m\frac{V_{3b}}{m_f}Da_{no}[NO]_{eql} \tag{14}$$

Another limiting case of interest consists of adequate time for zone 2 decomposition with dominant N_2O kinetics ($k_{1r} \rightarrow 0$), the most likely case for decomposition as shown by Mellor et al. (1998). For this situation, Eq. (13) reduces to

$$NO_xEI = m\frac{V_{3b}}{m_f}Da_{3b,4r}^{-1}[NO]_{eql} \tag{15}$$

where the kinetic time in $Da_{3b,4r}$ is evaluated at T_{3b}.

1.6 APPLICATION OF NO_X KINETIC MODEL TO DI DIESELS

1.6.1 Determining Significance of NO Decomposition in Diesel Engines

The ratio of the characteristic times for NO decomposition and formation, $\tau_{3b,no}/\tau_{no}$, provides a method to evaluate the importance of the former in any engine situation. This ratio is developed and verified in Mellor et al. (1998). The advantages of using this ratio are its ease of calculation and that it depends only on the fuel and engine operating parameters: engine load, pressure at SOC (P_2), temperature at SOC (T_2), compression ratio (r_c), and maximum cylinder pressure (P_3).

The effect of various engine operating parameters on the decomposition to formation time ratio is investigated by conducting an equilibrium analysis of various representative engine operating conditions for four DI Diesel engines. The engines examined (three heavy duty and one light duty) are relatively new engines, some of

which are equipped with state-of-the-art NO_x control systems (EGR and water injection). Configurations with turbocharging and inter/aftercooling as well as naturally aspirated are available. A complete table of engine descriptions is given in Mellor et al. (1998). The variety of engine setups gives a wide range of operating conditions from which to examine the results of the study.

Results of this investigation lead to the following conclusions about the effects of engine operating conditions on $\tau_{3b,no}/\tau_{no}$. By far the most important engine operating parameter affecting NO decomposition is load. The higher cylinder temperatures and pressures associated with higher loads increase the rate of decomposition. SOC and peak pressures, injection timing, and fuel properties have negligible effects. Start-of-combustion temperature and compression ratio have small influences masked by changes in load. Inert injection results can be interpreted in terms of their effect on equilibrium concentrations and characteristic temperatures in each zone.

1.6.2 Fluid Mechanic Mixing Times

The CTM equation for the prediction of engine-out NO_xEI is given in Eq. (13). In order to use this equation values for the fluid mechanic mixing times $\tau_{fi,no}$ and $\tau_{sl,3b}$ must be known. A characteristic mixing time can be defined as the time an eddy resides in a characteristic zone before its temperature is lowered to the point that the chemistry of interest is quenched by dilution or expansion. A primary assumption of the model construction done thus far has been that NO forms primarily in zone one and decomposes in zone two. Therefore, the characteristic fluid mechanic mixing time for NO formation ($\tau_{fi,no}$) is defined as the residence time of a stoichiometric eddy in zone 1. Likewise, the

characteristic mixing time for NO decomposition ($\tau_{sl,3b}$) is defined as the residence time of an eddy in zone 2.

Equation (13) includes both formation and decomposition reactions. Of the three unknowns in the equation, two are mixing times and one is a model constant. The model constant is equal to the slope of the linear best-fit line formed by graphing engine-out NO_xEI versus the appropriate model parameter. Thus, the constant can be solved for once the other two unknowns have been determined and is therefore ignored in the following analysis. The characteristic mixing time for NO decomposition is eliminated from the equation by utilization of low load engine data for which NO decomposition is thought to be negligible ($\tau_{no,3b} >> \tau_{no}$), thereby simplifying the equation to Eq. (14) with only $\tau_{fi,no}$ unknown.

Engine C data are used for the $\tau_{fi,no}$ study because these data contain a wide range of operating conditions at low load ($\tau_{no,3b} >> \tau_{no}$). Engine C is a HSDI Diesel with a displacement of 0.55 L/Cyl and is equipped with a turbocharger and intercooler. Mellor et al. (1998) give a full description of the engine. Analysis of Engine C data indicates that NO decomposition can be assumed negligible for loads of 600 kPa and below as discussed in Mellor et al. (1998).

An ongoing literature review gives insight as to which engine parameters should be included in the mixing time. Some of the topics being studied along with key references are listed in Table 1-1. This list is by no means thorough, but does give an idea of the mixing processes examined in the study.

Knowledge gained from the literature review about in-cylinder mixing is used to compile a list of mixing processes important to fuel-air mixing in the cylinder and the

characteristic terms by which they are modeled. Some such terms are: We_{air} – secondary breakup, Re_{air} – turbulence in air, etc. Using this list as a starting point, different

Table 1-1. Fluid Mechanic Research Topics

Effects of cylinder gas density on spray penetration and dispersion	Nabers and Siebers (1996), Arai and Hiroyasu (1990)
Fuel film formation and wall interaction	Stanton and Rutland (1996)
Engine speed	Uludogan et al. (1996)
Sauter mean diameter	Hiroyasu et al. (1989)
Secondary breakup	Arcoumanis et al. (1997)
Effects of swirl	Timoney and Smith (1996)
Overall combustion and/or mixing sources	Arcoumanis et al. (1997), Heywood (1988), Ferguson (1986)

definitions of the mixing time are tested to establish the best correlation between engine-out NO_xEI and the CTM model parameter.

A single $\tau_{fi,no}$ for all Engine C data, assuming NO decomposition negligible, has not yet been obtained. Instead, the data are correlated for the present using two separate empirical mixing times for NO formation. The first applies to cases in which fuel impinges on the cylinder bowl before SOC (wall jet), and the second to cases in which fuel impinges after SOC or not at all (free jet). The mixing times contain identical terms that are related to spray breakup, impingement time, and ignition delay time, but the significance (i.e. exponent) of each term is different for the two cases. The mixing time for the wall jet case is defined as

$$\tau_{fi,no} = \frac{We_{air}^{1.6}\, l_{imp}\, d_{noz}}{Re_{air}^{1.8}\, Re_{fuel}^{0.5}\, \upsilon_{fuel}} \left(\frac{\tau_{imp}}{\tau_{id}}\right)^{-0.5} \tag{16}$$

and the mixing time for the free jet case is found to be

$$\tau_{fi,no} = \frac{We_{air}^2 \, l_{imp} \, d_{noz}}{Re_{air}^{1.6} \, Re_{fuel}^{0.8} \, \upsilon_{fuel}} \left(\frac{\tau_{imp}}{\tau_{id}}\right)^{0.6} \quad (17)$$

Graphs of NO_xEI versus the right hand side of Eq. (14) can be found in Fig. 1-3 and 1-4. These graphs use data that meet the criteria of negligible decomposition (load ≤ 600kPa) and SOC = 0. The linear best-fit lines give correlation coefficient, R, values of 0.9793 and 0.9704 for the impingement before SOC and impingement after SOC cases, respectively. A problem arises with these linear fits in that as τ_{no} goes to infinity the engine-out NO_x is expected to go to zero, but for both cases the y-intercept is relatively large. We are evaluating the method of defining τ_{no} at this time. The lowest engine-out NO_x datum points seem to indicate the expected y-intercept of zero, however. The graphs presented are preliminary and appropriate fits will be determined after further research.

Currently, our efforts are directed toward improving the empirical mixing times for NO formation. We are hopeful that a single mixing time for NO formation can be found that is valid for start of combustion prior to and following wall impingement. Once a correctly defined mixing time for NO formation is developed for engine C, it will be validated for other engines. With a satisfactory definition of the mixing time for NO formation, work will begin on the mixing time for NO decomposition. When both mixing times have been defined the CTM will be capable of predicting NO_xEI for any DI Diesel operating condition.

1.7 CHARACTERISTIC TIME MODEL FOR SOOT FROM DIESEL ENGINES

Although the model for soot emissions is in the early stages of development, it is postulated that a two-zone model representing the formation and oxidation of soot will

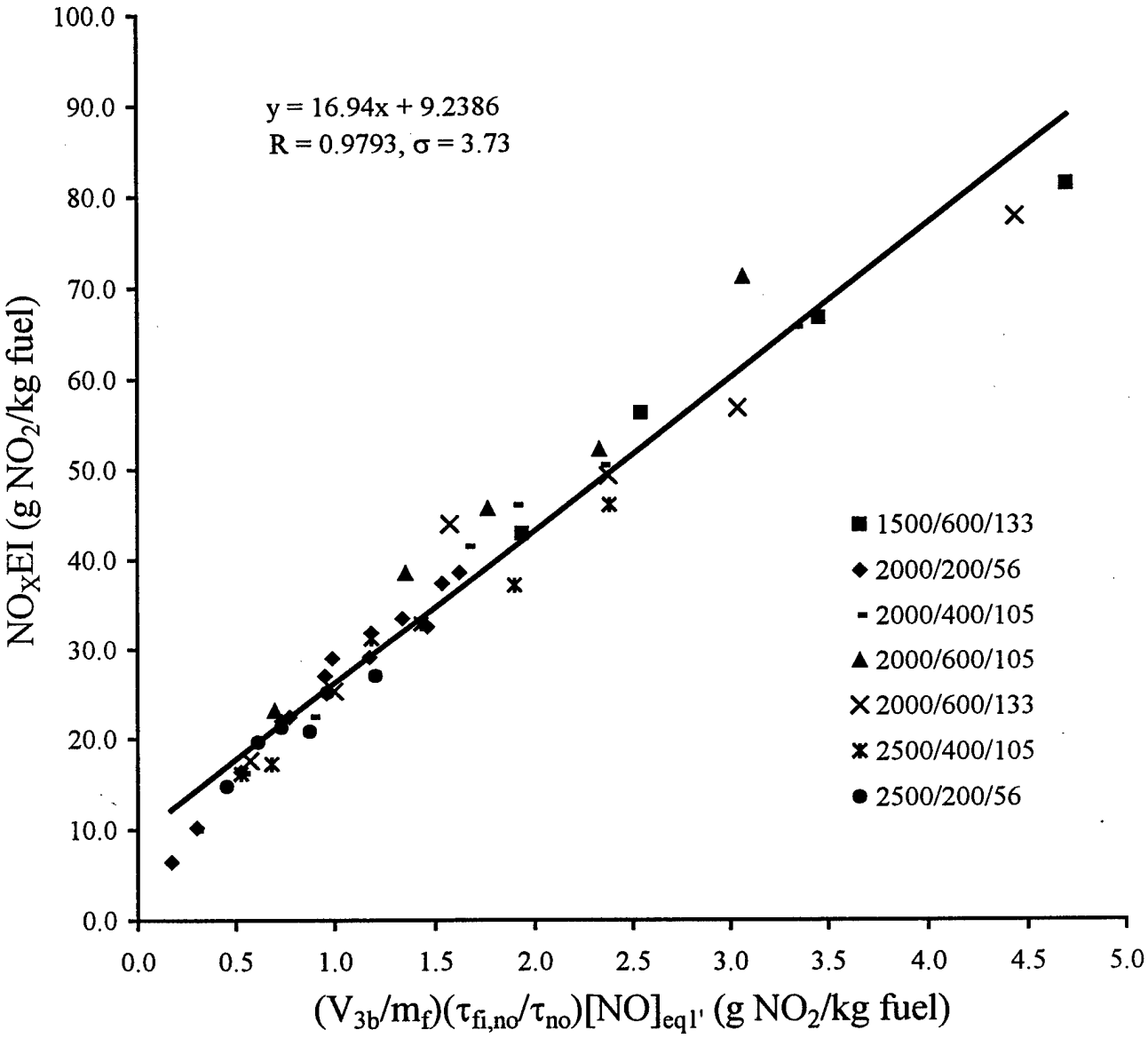

Figure 1-3. Engine-out NO_X emissions index versus model parameter (Eq. (14)) for wall jet datum points with SOC = 0. The legend has the format: engine speed (RPM)/load (kPa)/injection pressure (MPa). Each set of data is obtained via an EGR sweep.

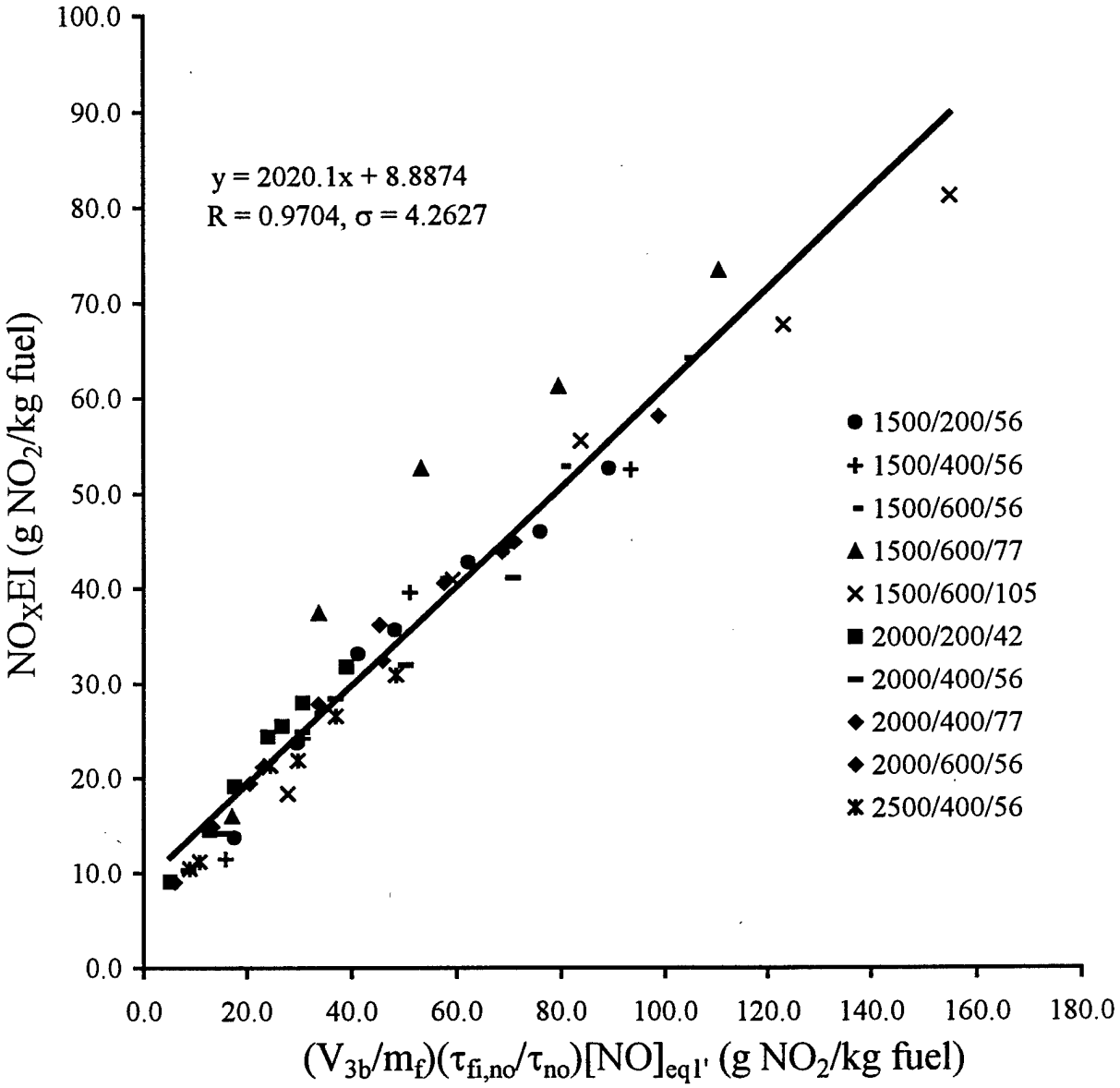

Figure 1-4. Engine-out NO_x emissions index versus model parameter (Eq. (14)) for free jet datum points with SOC = 0. The legend has the format: engine speed (RPM)/load (kPa)/injection pressure (MPa). Each set of data is obtained via an EGR sweep.

properly model this exhaust emission. Figure 1-5, based on past laser sheet images (see Dec, 1997), shows a schematic of a Diesel spray plume with the pertinent zones where soot is forming and oxidizing. Dec (1997) postulates that during the diffusion flame (mixing controlled) combustion, a thin premixed flame will form at the liquid/vapor fuel interface, and initiation of soot occurs just downstream of this flame in the products of rich combustion. Soot will then continue to form in the vapor fuel core, where a hypothetical homogeneous mixture with $\phi \approx 3$ exists, until it reaches the diffusion flame front. Thus, soot formation is assumed to occur spatially in the vapor core of the spray, labeled zone 1 in Fig. 1-5. For the oxidation of soot, Dec (1997) shows that due to the large concentrations of hydroxyl (OH) radicals in the diffusion flame, the majority of soot oxidation will occur in this location. This assumption is further supported through the work of Dec and Coy (1996) and Kosaka et al. (1995). For modeling purposes, it will be assumed that soot oxidation is initiated at the stoichiometric contour of the fuel spray and continues out into the periphery of the flame (see Fig. 1-5).

The representative temperature of zone 1, T_{sf}, is defined as an average of 2 limiting temperatures, namely the 50% fuel recovery temperature, $T_{50\%}$, and the $\phi=3$ flame temperature, $T_{\phi=3}$, where $T_{\phi=3}$ is calculated using TDC cylinder conditions as done for $T_{\phi=1}$. The temperature indicative of zone 2, T_{so}, is defined as the average of the stoichiometric and end of combustion temperatures, $T_{\phi=1}$ and T_{3b}.

Assuming the presence of soot formation and oxidation, the emissions model for soot was developed following the approach used by Mellor et al. (1998) to derive the NO_x CTM, except that global reactions for soot formation and oxidation will be used instead of a skeletal mechanism because of the complex chemistry involved in the

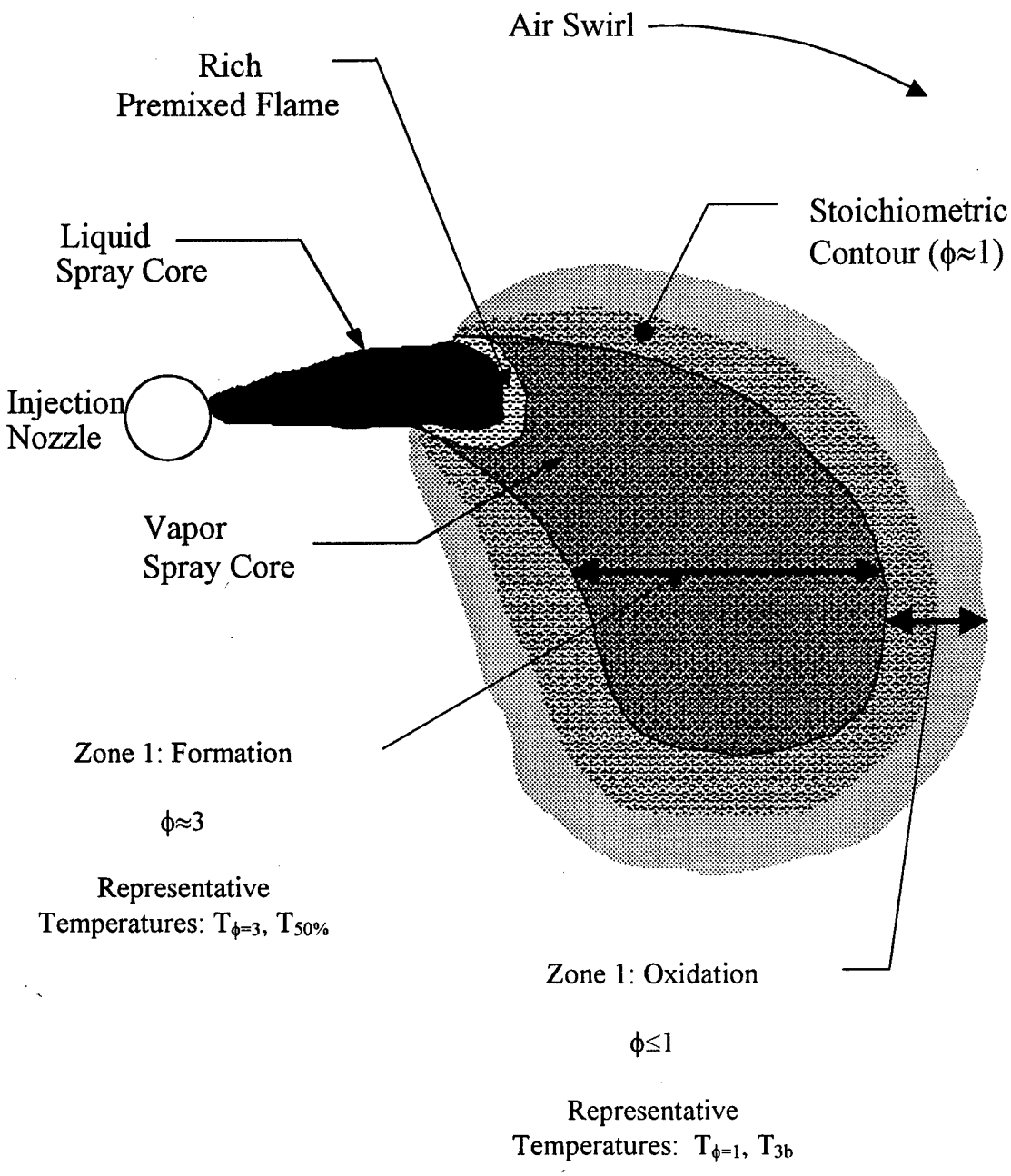

Figure 1-5. Schematic of a DI Diesel spray plume with regions of soot formation and oxidation labeled.

formation and oxidation of soot. This is consistent with the work of others to model soot emissions from Diesel engines (see for example, Nishida and Hiroyasu, 1989).

Following the methodology used in developing the NO_x CTM, the overall reactions used to model soot formation and oxidation are as follows:

$$\text{Fuel} \rightarrow \text{Soot} \tag{18}$$

$$\text{Soot} + \text{OH} \rightarrow \text{CO}_2 \tag{19}$$

Applying the law of mass action to Eqs. (18) and (19) gives

$$\left.\frac{d[\text{soot}]}{dt}\right|_{\text{form}} = k_{sf}[\text{fuel}] \tag{20}$$

$$\left.\frac{d[\text{soot}]}{dt}\right|_{\text{oxid}} = -k_{so}[\text{soot}]\cdot[\text{OH}] \tag{21}$$

In Eq. (20) it is assumed that soot has a first order of dependence on fuel. Now integrating Eqs. (20) and (21) over the lifetime that eddies spend in the soot formation and oxidation zones, $\tau_{sl,sf}$ and $\tau_{sl,so}$, respectively, yields

$$\frac{[\text{soot}]_1}{[\text{fuel}]} = m_{sf}\frac{\tau_{sl,sf}}{\tau_{sf}} = m_{sf}\cdot Da_{sf} \tag{22}$$

$$\frac{[\text{soot}]_2}{[\text{soot}]_1} = e^{-m_{so}\frac{\tau_{sl,so}}{\tau_{so}}} = e^{-m_{so}Da_{so}} \tag{23}$$

where $\tau_{sf} = 1/k_{sf}$, $\tau_{so} = 1/k_{so}[\text{OH}]$, and m_{sf} and m_{so} are model constants. For Eq. (23) it is assumed that [OH] is in steady state, which is based on the work of Tuttle et al. (1977) for the CO CTM. However, further development of this model by Connors et al. (1996) incorporates a first order dependence of [OH]. The concentrations $[\text{soot}]_1$ and $[\text{soot}]_2$ in Eq. (23) represent the amount of soot formed in zone 1 and the total soot remaining after

oxidation in zone 2 has ceased, where the amount $[soot]_2$ is dependent on the soot formed in zone 1.

The kinetic times associated with each of the chemical processes will be represented as inverse Arrhenius expressions:

$$\tau_x \sim \exp(E_x/RT_x) \tag{24}$$

with E_x and T_x the global activation energy and representative temperature, respectively, for each process.

The engine-out soot, in units of emissions index of soot, is obtained by combining Eqs. (22) and (23):

$$\text{SootEI} \propto \frac{[soot]_2}{[fuel]} = m_{sf} Da_{sf} \cdot e^{-m_{so} Da_{so}} \tag{25}$$

The soot model, Eq. (25), includes the competition between soot formation and oxidation with each process represented by the Damköhler numbers Da_{sf} and D_{so}, respectively.

Tuttle et al. (1977) showed the exponential term in the CO CTM, similar to that in Eq. (25), can be approximated by a series expansion of $\tau_{so}/\tau_{sl,so}$:

$$e^{-m_{so}\tau_{sl,so}/\tau_{so}} \approx a_0 + a_1 \frac{\tau_{so}}{\tau_{sl,so}} + a_2 \left(\frac{\tau_{so}}{\tau_{sl,so}} \right)^2 + \ldots \tag{26}$$

where the coefficients a_0, a_1, a_2 ... are determined through best fitting. Furthermore, Tuttle et al. (1977) found that neglecting the squared and higher terms for their measurements results in errors of less than one percent. If the same holds true for soot data, then the exponential term in Eq. (25) can be represented by the two term expansion resulting in the following:

$$\text{SootEI} \propto m_{sf} Da_{sf} \left(a_o + a_1 \frac{\tau_{so}}{\tau_{sl,so}} \right) \tag{27}$$

Equation (27) represents the final soot model, where the coefficient m_{sf} is determined from the best-fit slope of experimental data of SootEI plotted versus Da_{sf} times the bracketed term. Although Eq. (27) is preliminary, a point of departure would be to assure that the combination of both the NO_x and soot models is capable of predicting the trends existing between these exhaust emissions under various engine operating conditions.

1.8 NO_X – SOOT EMISSION TRENDS

1.8.1 Diesel Engine Performance

Since the Diesel engine is used in a number of applications, from large, heavy-duty (HD) engines for the military in combat vehicles to the smaller light-duty (LD) Diesels in small trucks and automobiles, performance requirements demand engine operation over wide load and speed cycles. The transient conditions under which commercial vehicles operate require Diesel engines to typically run at three quarter to full load (see Mori, 1997), while military vehicles spend the majority of time at low load conditions. These different load cycles result in different engine performance requirements which in turn lead to changes in the trends existing between NO_x and soot emissions.

Since any emissions model must be capable of predicting the changes in trends of exhaust emissions with varying engine operating conditions, examination of a performance map for DI Diesel engines is beneficial. Figure 1-6, a typical performance map, describes the effects of load and speed variations on bsfc (Heywood, 1988). The performance map shows that at approximately 50% load and speed, the best fuel economy of the engine is obtained. Note for the engine of Fig. 1-6, the maximum attainable load is limited to about 800 kPa bmep due to the smoke limit of the engine.

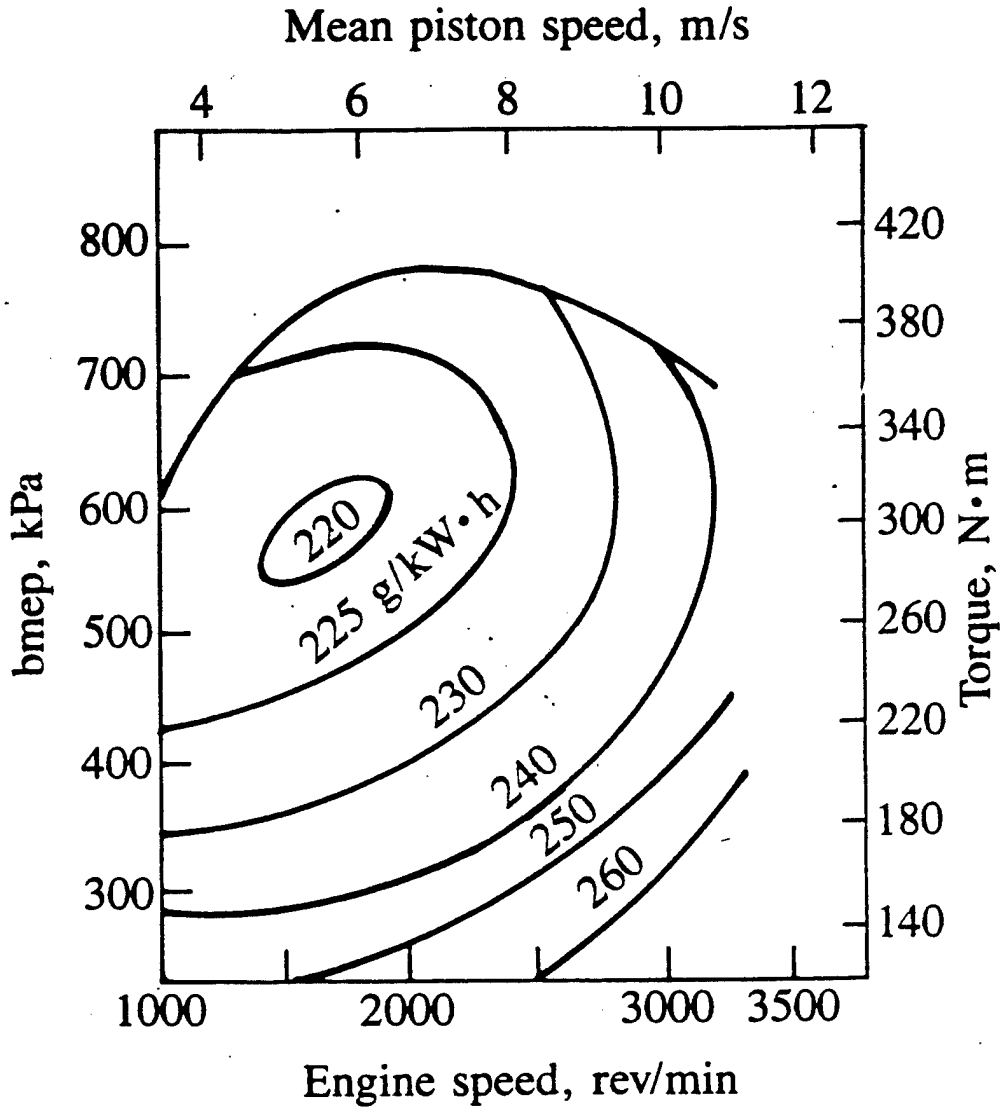

Figure 1-6. Performance map for a naturally aspirated DI Diesel engine (Heywood, 1988).

The Blue Ribbon Committee Report (BRC, 1995) shows the tradeoff between load (bmep) and bsfc through the relationship to the power density of a Diesel engine (ρ_d), defined as the engine output divided by the volume of the engine plus accessories (i.e., turbocharger, air filter, etc.):

$$\rho_d \propto \text{bmep} \propto (\rho_a)(\phi)(1/\text{bsfc}) \tag{28}$$

where ρ_a is the cylinder inlet air density and ϕ the equivalence ratio. From Eq. (28), the highest ρ_d would be obtained by a turbocharged (increased ρ_a) engine operating under rich conditions with low bsfc; however, rich operating conditions will result in higher particulate and bsfc (BRC, 1995). The tradeoff in Eq. (28) between bmep and bsfc translates into different trends existing between NO_x and soot.

The work of Wilson et al. (1973) and Murayama et al. (1978) clearly exhibits the effects that increasing load has on bsfc and emissions of soot and NO_x for a constant speed. As the load (or ϕ) is increased, NO_x and soot emissions simultaneously increase until a maximum value of NO_x is reached, after which a further increase in load yields a decrease in NO_x and a continued increase in soot. The initial increase in NO_x with load corresponds to the decrease in bsfc; once the minimum in bsfc is obtained, roughly coinciding with the maximum NO_x, any further increase in load results in a decrease in NO_x that is caused not only by the increase in bsfc, but also extended burning into the expansion stroke causing reductions in peak gas temperature and increased heat losses so the production rate of NO is reduced, according to Wilson et al. (1973). As discussed in the previous sections, an alternative interpretation of the results involves increased decomposition of NO as load is increased.

The above discussion suggests that there are two different trends present between NO_x and soot emissions with varying load: 1) low load cases ($\leq$ 50% load) show an increase in NO_x and soot with increasing load and 2) higher load cases ($\geq$50%) where the typical NO_x/soot tradeoff exists. Algegraic expressions are derived below from the NO_x and soot CTMs to prove that the overall model will properly predict the trends of NO_x and soot emissions, regardless of operating conditions.

1.8.2 Derivation of NO_x - Soot Trends Using the CTM

To derive the NO_x/soot emissions equations for Diesel engines, a relationship between the NO_x and soot CTM is needed. The link in the derivation is the mixing times involved in the models for NO_x and soot emissions. The zonal assumptions of the NO_x and soot CTMs indicate that NO is forming at the diffusion flame front, which as noted previously is the same spatial region for soot oxidation initiation. Therefore, a possible relationship between these two mixing times may exist and could be used in the derivation of the NO_x/soot tradeoff equations.

Analysis of the Engine C data[†] leads to an expression for the mixing time associated with NO formation, $\tau_{fi,no}$, where NO_x has a first order dependence with pressure drop, ΔP, across the injection nozzle, and a -1.6 order of dependence with engine speed (Eq. 17). A similar analysis for Engine C soot data was performed to determine the dependency of soot with each of the above operating parameters; however, the chemical kinetics for the soot model are not yet fully developed, so engine conditions must be such that only the engine parameter of interest (i.e., ΔP or N) is varying. For

[†] Analysis only includes data where NO decomposition is negligible (200-600 bmep range) and the injected fuel ignites prior to impinging on the piston bowl wall (free jet).

example, soot data for constant load, EGR and injection pressure were used to determine the order of dependence of soot with engine speed. The results show that soot has an approximate third order dependence with engine speed, which is twice the inverse of that found for NO_x and slightly higher than the value used by Plee et al. (1981). There is no single order dependence of soot on ΔP; instead the magnitude of dependence varies with EGR (i.e., increasing EGR decreases the order dependence). However, in general the analysis did reveal that soot emissions will have an inverse dependency on ΔP, opposite the dependency found for NO_x, which is expected.

Several major issues arose during the above analysis of the soot emissions from Engine C. The first problem was that the yet-to-be-determined chemical kinetics for soot formation and oxidation act as a constraint and eliminate many datum points since only ΔP or N variations can be considered, while load, EGR, and SOC are constant. Thus, more datum sets with only ΔP or N changing are needed in order to ensure that the obtained dependencies of soot with ΔP and N are well understood. Another issue concerning the available data is the lack of high load run conditions. These higher load data are required to test and ensure that the CTM will properly predict soot over the entire load cycle, not just at low loads.

Although there exist some questions about the data available for analysis, the overall trends of soot emissions with ΔP and speed are consistent with those reported by Plee et al. (1981); therefore, the NO_x/soot proportionality can be derived for these data. In general, it has been shown that soot has an inverse and perhaps a higher order of dependence on ΔP and N than found for NO_x. These results would suggest the mixing times associated with soot oxidation and NO formation are inversely proportional:

$$\tau_{fi,no} \propto \frac{1}{\tau_{sl,so}} \tag{29}$$

By solving for $\tau_{fi,no}$ and $\tau_{sl,so}$ in Eqs. (14) and (27), respectively, and substituting these new expressions into Eq. (29), the following NO_x/soot equation is obtained:

$$NO_x EI \propto \frac{SootEI}{a_1 m_{sf} Da_{sf} \tau_{so}} - \frac{a_0}{a_1 \tau_{so}} \tag{30}$$

Equation (30) shows that the NO_x and soot emissions are directly proportional for the lower load data, which is consistent with the trends shown by Wilson et al. (1973) and Murayama et al. (1978). Higher load data will be required to determine the relationship existing between the mixing times associated with NO_x and soot emissions. The higher load data are expected to exhibit the NO_x/soot tradeoff obtained through "normal" vehicle operation.

2.0 PUBLICATIONS AND TECHNICAL REPORTS

Duffy, K.P. and Mellor, A.M. (1995), "Characteristic time model for Diesel particulate emissions," Interim Technical Report, US Army Research Office.

Duffy, K.P., Nicols, J.T., Mellor, A.M. and Plee, S.L. (1996), "Flame temperature correlations for effects of EGR in high speed Direct Injection Diesel engines," Proceedings of the 1996 Technical Meeting of the Central States Section of the Combustion Institute.

Psota, M.A. and Mellor, A.M. (1996), "Water injection effects on NO_x emissions for engines utilizing nonpremixed combustion," Proceedings of the 1996 Technical Meeting of the Eastern States Section of the Combustion Institute.

Psota, M.A., Easley, W.L., Fort, T.H. and Mellor, A.M. (1997), "Water injection effects on NO_x emissions for engines utilizing diffusion flame combustion," SAE Paper 971657.

Mellor, A.M., Mello, J.P., Duffy, K.P., Easley, W.L. and Faulkner, J.C. (1998), "Skeletal mechanism for NO_x chemistry in Diesel engines," SAE Paper 981450.

Various Internal Ford Reports, Ford Motor Company, Dearborn, MI.

3.0 PARTICIPATING PERSONNEL

Mellor, A.M., Centennial Professor, Mechanical Engineering Department, Vanderbilt University, Nashville, TN.

Plee, S.L., Director, Systems Engineering, Motorola, Inc., Dearborn, MI.

Tabaczynski, R.J., Director, Powertrain and Vehicle Research Laboratory, Scientific Research Laboratories, Ford Motor Company, Dearborn, MI.

Duffy, K.P., Ph.D. Candidate.

Gurtner, D., M.S.

Mello, J.P., M.S. Candidate.

Easley, W.L., M.S. Candidate.

Psota, M.A., M.S. Candidate.

A number of undergraduate students participated throughout the program as well.

4.0 REPORT OF INVENTIONS

No inventions were made under the sponsorship of the grant.

5.0 REFERENCES

Ahmad, T. and Plee, S.L. (1983), "Application of flame temperature correlations to emissions from a direct injection Diesel engine," SAE Paper 831734.

Arcoumanis, C., Gavaises, M. and French, B. (1997), "Effect of fuel injection processes on the structure of Diesel sprays," SAE Paper 970799.

Blue Ribbon Committee (BRC, 1995), "Research needed for more compact intermittent combustion propulsion systems for Army combat vehicles," Vol. I, Executive Summary and Main Body; Vol. II, Appendices, Southwest Research Institute, San Antonio, Texas.

Bowman, C.T., Hanson, R.K., Davidson, D.F., Gardiner, W.C., Lissianski, V., Smith, G.P., Golden, D.M., Frenklach, M. and Goldenberg, M. (1995), http://www.me.berkeley.edu/gri_mech/

Connors, C.S., Barnes, J.C. and Mellor, A.M. (1996), "Semi-empirical predictions and correlations of CO emissions from utility combustion turbines," Journal of Propulsion and Power, Vol. 12, No. 5, 926-935.

Dec, J.E. (1997), "A conceptual model of DI Diesel combustion based on laser-sheet imaging," SAE Paper 970873.

Dec, J.E. and Coy, E.B. (1996), "OH radical imaging in a DI Diesel engine and the structure of the early diffusion flame," SAE Paper 960831.

Fenimore, C.P. (1971), "Formation of nitric oxide in premixed hydrocarbon flames," Thirteenth Symposium (International) on Combustion, The Combustion Institute, Pittsburgh, 373-380.

Ferguson, C.R. (1986), Internal Combustion Engines, Applied Thermosciences, John Wiley & Sons, New York.

Heywood, J. B. (1988), Internal Combustion Engine Fundamentals, McGraw-Hill, Inc., New York.

Hiroyasu, H., Arai, M. and Tabata, M. (1989), "Empirical equations for the Sauter mean diameter of a Diesel spray," SAE Paper 890464.

Lavoie, G. A., Heywood, J.B. and Keck, J.C. (1970), "Experimental and theoretical investigation of nitric oxide formation in internal combustion engines," Combust. Sci. Tech. 1, 313-326.

Kosaka, H., Nishigaki, T. and Kamimoto, T. (1995), "A study on soot formation and oxidation in an unsteady spray flame via laser induced incandescence and scattering techniques," SAE Paper 952451.

Malte, P.C. and Pratt, D. T. (1974), "The role of energy-releasing kinetics in NO_x formation: fuel lean, jet-stirred CO-air combustion," Combust. Sci. Tech. 9, 221-231.

Mellor, A.M., Mello, J.P., Duffy, K.P., Easley, W.L. and Faulkner, J.C. (1998), "Skeletal mechanism for NO_x chemistry in Diesel engines," SAE Paper 981450.

Mori, K. (1997), "Worldwide trends in heavy-duty Diesel engine exhaust emission legislation and compliance technologies," SAE Paper 970753.

Murayama, T., Morishima, Y., Tsukahara, M. and Miyamoto, N. (1978), "Experimental reduction of NO_x, smoke, and BSFC in a Diesel engine using uniquely produced water (0 – 80%) to fuel emulsion," SAE Paper 780224.

Naber, J.D. and Siebers, D.L. (1996) "Effects of gas density and vaporization on penetration and dispersion of Diesel sprays," SAE Paper 960034.

Nishida, K. and Hiroyasu, H. (1989), "Simplified three-dimensional model of mixture formation and combustion in a DI Diesel engine," SAE Paper 890269.

Plee, S., Ahmad, T., Myers, J. and Siegla, D. (1980), "Effects of flame temperature and air/fuel mixing on emission of particulate carbon from a divided chamber Diesel engine", Particulate Carbon: Formation During Combustion, Plenum Press, New York, pp. 423-483.

Plee, S. L., Ahmad, T. and Myers, J. P. (1981), "Flame temperature correlation for the effects of exhaust gas recirculation on Diesel particulate and NO_x emissions," SAE Paper 811195.

Sawyer, R.F., Cernansky, N.P. and Oppenheim, A.K. (1973), "Factors controlling pollutant emissions from gas turbine engines," Atmospheric Pollution by Aircraft Engines, AGARD CP No. 125.

Stanton, D.W. and Rutland, C.J. (1996), "Modeling fuel film formation and wall interaction in Diesel engines," SAE Paper 960628.

Timoney, D.J. and Smith, W.J. (1996), "Influences of fuel injection and air motion energy sources on fuel-air mixing rates in a DI Diesel combustion system," SAE Paper 960035.

Tuttle, J.H., Colket, M.B., Bilger, R.W. and Mellor, A.M. (1977), "Characteristic times for combustion and pollutant formation in spray combustion," Sixteenth Symposium (International) on Combustion, The Combustion Institute, Pittsburgh, 209-219.

Uludogan, A., Foster, D. E. and Reitz, R. D. (1996), "Modeling the effect of engine speed on the combustion process and emissions in a DI Diesel engine," SAE Paper 962056.

Wilson, R.P., Muir, E.B. and Pellicciotti, F.A. (1973), "Variables affecting pollutant emissions from a single-cylinder Diesel engine," Spring Technical Meeting of the Western States Section of the Combustion Institute.